Available online at www.sciencedirect.com
ScienceDirect
Applied Catalysis B: Environmental 78 (2008) 301–308
APPLIED CATALYSIS B: ENVIRONMENTAL
www.elsevier.com/locate/apcatb

SO_2 resistant antimony promoted V_2O_5/TiO_2 catalyst for NH_3-SCR of NO_x at low temperatures

Ha Heon Phil *, Maddigapu Pratap Reddy, Pullur Anil Kumar, Lee Kyung Ju, Jung Soon Hyo

Functional Materials Research Center, Korea Institute of Science and Technology, Cheongryang, Seoul 130-650, Republic of Korea

Received 28 June 2007; received in revised form 7 September 2007; accepted 12 September 2007
Available online 19 September 2007

Abstract

To get the low temperature sulfur resistant V_2O_5/TiO_2 catalysts quantum chemical calculation study was carried out. After selecting suitable promoters (Se, Sb, Cu, S, B, Bi, Pb and P), respective metal promoted V_2O_5/TiO_2 catalysts were prepared by impregnation method and characterized by X-ray diffraction (XRD) and Brunner Emmett Teller surface area (BET-SA). Se, Sb, Cu, S promoted V_2O_5/TiO_2 catalysts showed high catalytic activity for NH_3 selective catalytic reduction (NH_3-SCR) of NO_x carried at temperatures between 150 and 400 °C. The conversion efficiency followed in the order of Se > Sb > S > V_2O_5/TiO_2 > Cu but Se was excluded because of its high vapor pressure. An optimal 2 wt% 'Sb' loading was found over V_2O_5/TiO_2 for maximum NO_x conversion, which also showed high resistance to SO_2 in presence of water when compared to other metal promoters. In situ electrical conductivity measurement was carried out for Sb(2%)/V_2O_5/TiO_2 and compared with commercial W(10%)V_2O_5/TiO_2 catalyst. High electrical conductivity difference (ΔG) for Sb(2%)/V_2O_5/TiO_2 catalyst with temperature was observed. SO_2 deactivation experiments were carried out for Sb(2%)/V_2O_5/TiO_2 and W(10%)/V_2O_5/TiO_2 at a temperature of 230 °C for 90 h, resulted Sb(2%)/V_2O_5/TiO_2 was efficient catalyst. BET-SA, X-ray photoelectron spectroscopy (XPS) and carbon, hydrogen, nitrogen and sulfur (CHNS) elemental analysis of spent catalysts well proved the presence of high ammonium sulfate salts over W(10%)/V_2O_5/TiO_2 than Sb(2%)/V_2O_5/TiO_2 catalyst.

Keywords: NO_x conversion at low temperature; Sb(2%)/V_2O_5/TiO_2; Electrical conductivity; Resistance to SO_2

1. Introduction

Nitrogen oxides (NO_x) emitted from automobiles and stationary sources such as oil and coal-fried power plants, waste incinerators, industrial ovens and chemical processes. Nearly all NO_x (95%) derives from transportation (49%) and power plants (46%) [1]. They contribute to photochemical smog, acid rain, ozone depletion and greenhouse effects. The direct health hazards related to NO_x are bronchitis, pneumonia, viral infections and hay fever. Selective catalytic reduction (SCR) of NO_x to N_2 using ammonia as a reductant is now considered to be the most effective and common technique to remove the NO_x in the exhaust gas from stationary sources [2,3]. The general reaction occurring is

$$4NO + 4NH_3 + O_2 \rightarrow 4N_2 + 6H_2O.$$

The well known industrial catalyst for this process is based on V_2O_5/TiO_2 (anatase) promoted with WO_3. The required operating temperature for the above industrial catalyst is typically 300–400 °C. This makes it necessary to locate the SCR unit upstream of the desulfurizer and/or particulate control device in order to avoid reheating the flue gas. Despite the low sensitivity of this catalyst to SO_2 poisoning, deactivation does occur. The life of the catalyst is shortened because of high concentrations of SO_2 and ash in the flue gas. This can be avoided by locating the SCR unit at the very end of the flue gas pollution abatement units where the flue gas is relatively clean as it passes through the scrubber and the electrostatic precipitator or bag-house. Therefore, in certain circumstance where flue gas temperature is low, it is necessary to develop a catalyst which shows high activity at a lower reaction

* Corresponding author. Tel.: +82 2 958 5461; fax: +82 2 958 5379.
E-mail address: heonphil@kist.re.kr (H.H. Phil).

0926-3373/$ – see front matter © 2007 Elsevier B.V. All rights reserved.
doi:10.1016/j.apcatb.2007.09.012

temperature. A low temperature SCR process is believed to have low energy consumption and to be economical for retrofitting into the existing units for flue gas cleaning. The key to development of the low temperature SCR process is SCR catalysts of high resistance to SO_2 poisoning because the formation of the ammonium bisulfate salts on the catalyst surface is serious at low temperatures [4].

Several types of low temperature active catalysts have been developed [5–8]. However, they have poor durability under sulfur and water environments. Some supported transition metal oxide catalysts have been investigated for the low temperature SCR reactions, which are capable of operating at the low temperature range between 80 and 250 °C. Amorphous chromia [9], carbon-supported vanadium [10,11], manganese [12] and copper [5,6] oxides, alumina supported manganese oxide [13], TiO_2 supported chromia [14], vanadium and copper-nickel oxides supported on titania and alumina monoliths [15], show high activity for NO reduction with NH_3 at low temperatures. Peña et al. [16] reported that the catalytic performance of titania supported V, Cr, Mn, Fe, Co, Ni and Cu catalysts followed the order of Mn > Cu > Cr > Co > Fe > V > Ni for low temperature (80–250 °C) SCR of NO with NH_3. These catalysts have the drawback of SO_2 poisoning in the presence of water and it was reported that chemical transformation of MnO to $MnSO_4$ was the main reason for deactivation of SCR over MNO_x/Al_2O_3 [17].

Generally, when titanium dioxide (TiO_2) supporters and vanadium (V) used as active catalytic materials, the additional amount of vanadium is added to increase the catalytic activity at 300 °C or lower. However, when the amount of vanadium increased, the oxidation of sulfur dioxide (SO_2) to sulfur trioxide (SO_3) is induced, which further reacts with slipped ammonia. As a result ammonium bisulfate (NH_4HSO_4), a solid salt formed over the catalyst surface and interfere the SCR reaction. Hence the amount of unreacted ammonia increases, formation of sulfur trioxides (SO_3) is promoted, thereby accelerating the sulfur poisoning, which eventually shortens the life of the catalysts. Therefore, catalysts that can improve catalytic activity at low temperatures without promoting the oxidation of sulfur dioxides need to be developed.

In the case of V_2O_5/Al_2O_3 [18], formation of aluminum sulfate during SCR reaction in the presence of SO_2 reduces surface area of the catalyst sorbents, which results in severe deactivation of SCR activity. NH_4HSO_4 was also found to accumulate on the surface of V_2O_5/TiO_2 [19,20], V_2O_5/AC [21,22], and CuHM [23] at temperatures below 280 °C which inhibits SCR activity due to pore plugging. Conventionally, in order to enhance low temperature activity and sulfur poisoning resistance, tungsten has been added to V_2O_5/TiO_2 catalysts as a promoter [19,24–26]. When tungsten (W) used as promoter it could be important to increase the percentage of tungsten approximately 5–10 wt% to get the low temperature sulfur poisoning resistance. However, the amount of tungsten increases the price of the catalyst. Our aim is to find a promoter which can replace tungsten as well as to improve the sulfur poisoning at low temperatures.

In the present study, quantum chemical calculation was carried out to choose promoters which can replace tungsten. In situ electrical conductivity studies were carried out for the promoted V_2O_5/TiO_2 catalysts before and after the exposure of mixture gas and difference in the electrical conductivity (ΔG) values were correlated with the NO_x conversion efficiencies. SO_2 deactivation experiments with time on stream were also carried for the catalysts chosen and compared with commercial $W(10\%)/V_2O_5/TiO_2$ catalyst. X-ray photoelectron spectroscopy (XPS), Brunner Emmett Teller surface area (BET-SA) and carbon, hydrogen, nitrogen and sulfur (CHNS) elemental analysis were carried out to analyze the presence of ammonium bisulfate salt which is main cause for SO_2 poisoning effect.

2. Experimental

2.1. Quantum chemical studies

Adsorption of ammonium bisulfate on the V_2O_5/TiO_2 promoted by metal (M) was modeled as described in Fig. 1. Quantum chemical calculation was carried out using indigenous Spanish initiative for electronic simulations with thousands of atoms (SIESTA) software to estimate bonding strengths between ammonium bisulfate and transition metals. From this quantum chemical calculations the best metals which have weak bond strength were screened from the periodic table and selected for the NH_3-SCR to reduce the low temperature sulfur dioxide deactivation caused by the formation of ammonium bisulfate salts over metal promoted V_2O_5/TiO_2 catalyst.

2.2. Catalyst preparation

The commercial TiO_2 (DT-51 Millennium Chemicals) powder was used as support for the preparation of all catalysts. The V_2O_5/TiO_2 catalyst was prepared by wet impregnation of vanadia on titania by using ammoniummetavanadate (NH_4VO_3) (99% pure Junsei chemicals) precursor. The required amount of ammoniummetavanadate was added to the oxalic acid solution and heated to dissolve ammoniummetavanadate. To this solution the calculated amount of titania (DT-51) powder was added and stirred for an hour followed by evaporation, drying and calcination at 400 °C for 4 h in air. Following the same procedure a series of MO_x-V_2O_5/TiO_2 catalysts were prepared by

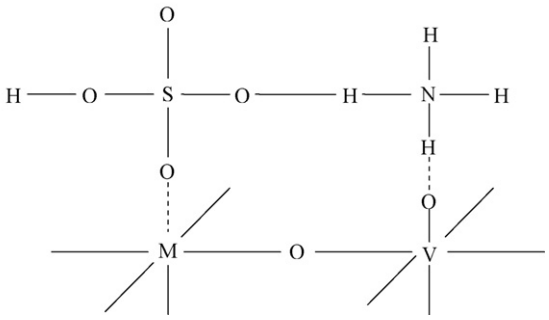

Fig. 1. Modeling for the adsorption of ammonium bisulfate over V_2O_5-MO_x/TiO_2.

using different metal (Se, Sb, Cu, S, B, Bi, Pb and P) precursor salts (99% pure Aldrich chemicals). Commercial W(10%)/V_2O_5/TiO_2 catalyst supplied by Kerr McGee was used as it is.

2.3. Characterization

All the prepared catalysts were analyzed by powder X-ray diffractometer (XRD) (Bruker) and spectra were recorded using a Ni filtered Cu Kα radiation, operated at 40 kV and 20 mA. The fine powders were scanned in the 2θ range from 20 to 80. BET-SA of the prepared catalysts were measured from N_2 adsorption isotherms at −196 °C using a micromeritics (Autochem-II 2920) analyzer. X-ray photo electronic spectrographs (XPS) (recorded by using PHI 5800 ESCA system), BET-SA (Autochem-II 2920) and elemental analysis (by using Perkin-Elmer 2400 series II CHNS analyzer) were analyzed for the spent catalysts as post-characterization study.

2.4. Electrical conductivity measurements

The electrical conductivity (σ) measurements were carried under vacuum conditions using inbuilt setup (Fig. 2) consisting of a cell with platinum electrodes, thermocouple, heating coil and electrometer (Keithley 6517A) using following procedure: (a) 400 mg of the catalyst was loaded in between the circular platinum electrodes in the cell (b) evacuation of the cell and preheating of the catalyst was carried to remove the water and physically adsorbed gases at 150 °C for 2 h (c) after cooling to room temperature, 400 cm^3 of pure oxygen gas (5.5×10^2 Pa) was introduced and maintained the desired reaction temperature with a ramp of 5 °C min^{-1} (e) evacuation of the cell was done and electrical conductivity (σ) of the loaded catalyst were measured by introducing pure reactant gases into the cell at the respective reaction temperatures using the formula [27]

$$\sigma = \frac{t}{RS}$$

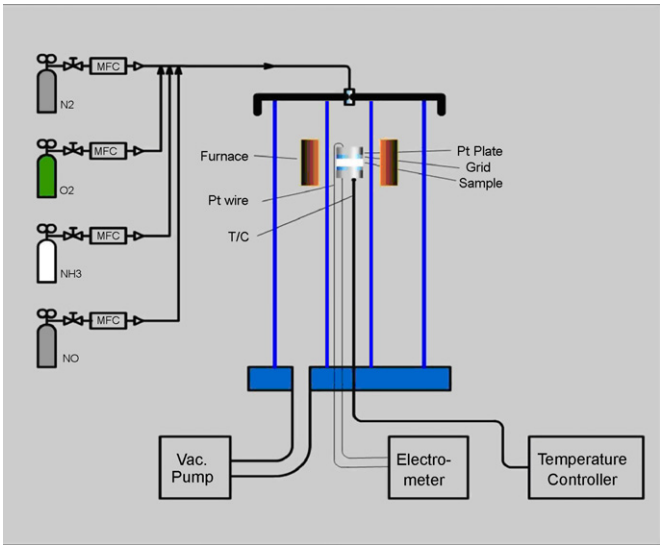

Fig. 2. Diagram of electrical conductivity measurement unit.

where σ is the conductivity, t the thickness of the loaded catalyst between circular platinum electrodes, R the resistance and S is the cross-sectional area of the circular platinum electrodes.

2.5. Activity measurements

Catalytic activity measurements were (carried with and without SO_2 in presence of water) performed in a dynamic online micro reactor using a feed stream consisting of 800 ppm NO_x, 800 ppm NH_3, 3 vol% O_2, 6 vol% H_2O, 500 ppm SO_2 and nitrogen balance in the temperature range between 150 and 400 °C, with a total flow rate of 500 cm^3 min^{-1} and at a space velocity of 60,000 h^{-1}. The catalysts particle size of 300–425 μm were used for activity measurements and about 250 mg of the catalyst was inserting into the middle of quartz tube supporting by quartz wool which was positioned middle of the reactor. The effluent from the reactor was analyzed by an online NDIR Fuji NO and SO_2 analyzer. NO conversion was calculated by using the formula given below. The sulfur deactivation studies with time on stream were also carried out and compared with commercial W(10%)/V_2O_5/TiO_2 catalyst at low temperatures.

$$\text{NO conversion} = \frac{NO_{in} - NO_{out}}{NO_{in}} \times 100$$

3. Results and discussion

3.1. Screening of metals by quantum chemical calculation

Quantum chemical calculation was carried out to estimate bonding strength between ammonium bisulfate and for the different metals in the periodic table. An adsorption model of ammonium bisulfate to V_2O_5/TiO_2 catalysts [28] was schematically shown in Fig. 1. The diagram shows the ammonium bisulfate adsorption on to the V_2O_5/TiO_2 surface where TiO_2 surface is covered by V_2O_5 and a transition metal where Ti is replaced with an arbitrary atom M. In the model, the bonding strength of M···O, which has normally stronger bond than adjacent H···O bond, plays a critical role on the sulfur poisoning. As the bonding strength becomes weaker (M···O), ammonium bisulfate salt can be easily desorbed. From the quantum chemical calculation, suitable metal promoters like Se, Sb, Cu, S, B, Bi, Pb and P were selected on the basis of bond energy (M···O) which may favors the weaker bonding strength (M···O), thus leads to easy desorption of adsorbed ammonium bisulfate salt formed during NH_3-SCR of NO_x reaction over the catalyst surface at low temperatures. Among all the selected metal promoters, the order of bonding energy decreased as Pb > B > Bi > Cu > Sb > Se > S > P (Table 1). Taking in to the consideration of order, the best candidate metals 'S' and 'P' showed too low NO_x reduction, and next candidate 'Se' showed very poor resistance to SO_2 deactivation because of its high vapor pressure at the reaction temperature. Next best candidate 'Sb' showed high activity as well as high resistance to SO_2 deactivation among all. This is further explained in detail coming sections.

Table 1
The quantum chemical calculation results

Element	Bond energy (eV)
Selenium (Se)	+2.940
Antimony (Sb)	+3.129
Copper (Cu)	+3.158
Sulfur (S)	+2.770
Boron (B)	+3.721
Bismuth (Bi)	+3.509
Lead (Pb)	+3.711
Phosphorous (P)	+2.501

3.2. Characterization

The prepared catalysts (Se, Sb, Cu, S, B, Bi, Pb and P doped V_2O_5/TiO_2) were characterized by XRD and BET-SA. The XRD spectra of all the catalysts showed the anatase TiO_2 phases at 2θ of 25.3, 38.0 and 48.0, but the V_2O_5 phases were not observed because of high dispersion and very low percentage (V_2O_5(2%)/TiO_2) of metal content used in preparation of catalysts. Similarly with the addition of promoters (1%) to the V_2O_5(2%)/TiO_2 it is observed that there is no change in the XRD patterns and no specific phases were observed corresponding to the promoters. The composition of the different promoters and V_2O_5 on TiO_2 and BET-SA of the all catalysts are given in Table 2. It could be seen that the highest surface area is obtained for the support TiO_2, the values changed with addition of the promoters to the V_2O_5/TiO_2 which is expected. XPS and CHNS elemental analysis were done for the spent catalysts after 90 h sulfur deactivation study and the observations were discussed further in Section 3.6.

3.3. Influence of promoters on SCR activity in the presence of oxygen

Fig. 3 shows the NO_x conversion of different metal promoted V_2O_5/TiO_2 catalysts with temperature. The activity was carried in the temperature range from 150 to 400 °C with the reaction mixture containing 800 ppm NO_x, 800 ppm NH_3, 3% O_2 at a space velocity of 60,000 h^{-1}. The results show that considerable increase in reaction rate at low temperatures (150–300 °C).

Table 2
Composition and BET-SA of the catalysts

Catalyst	Composition		BET-SA ($m^2\ g^{-1}$)
	V_2O_5 (%)	MO_x (%)	
TiO_2	–	–	94
V_2O_5/TiO_2	2	–	91
1% Se/V_2O_5/TiO_2	2	1	90
1% Sb/V_2O_5/TiO_2	2	1	91
2% Sb/V_2O_5/TiO_2	2	2	89
1% Cu/V_2O_5/TiO_2	2	1	87
1% S/V_2O_5/TiO_2	2	1	89
1% B/V_2O_5/TiO_2	2	1	85
1% Bi/V_2O_5/TiO_2	2	1	87
1% Pb/V_2O_5/TiO_2	2	1	87
1% P/V_2O_5/TiO_2	2	1	85

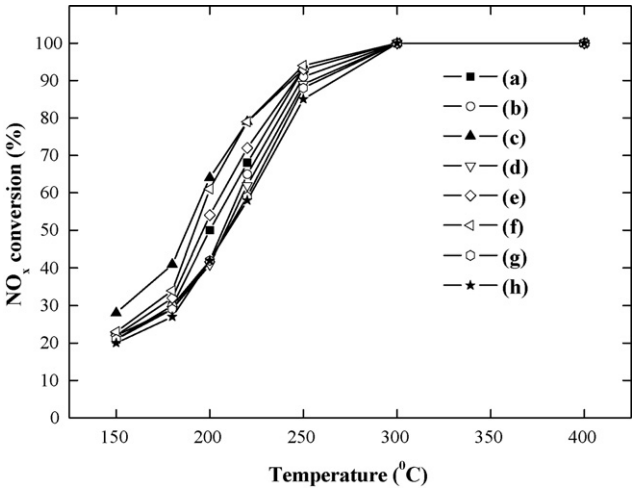

Fig. 3. NO_x conversion vs. temperature over (a) V_2O_5/TiO_2, (b) 1% Cu/V_2O_5/TiO_2, (c) 1% Se/V_2O_5/TiO_2, (d) 1% Pb/V_2O_5/TiO_2, (e) 1% S/V_2O_5/TiO_2, (f) 1% Sb/V_2O_5/TiO_2, (g) 1% B/V_2O_5/TiO_2 and (h) 1% P/V_2O_5/TiO_2 (conditions: 800 ppm NO_x, 800 ppm NH_3, 3 vol% O_2, S.V.—60,000 h^{-1}).

NO_x conversion of all catalysts increased with increasing temperature and achieved almost 100% NO_x conversion at 300 °C. The difference in the conversion was observed at low temperatures below 250 °C. Among all the catalysts, selenium (Se) showed the highest NO_x conversion at low temperatures and antimony (Sb) followed it. The low temperature NO_x conversions of Se, Sb, Cu and S promoted V_2O_5/TiO_2 catalysts followed Se > Sb > S > V_2O_5/TiO_2 > Cu order. The V_2O_5/TiO_2 catalyst obtained 50% conversion at a low temperature of 200 °C where as Se/V_2O_5/TiO_2 obtained 64% of conversion and Se/V_2O_5/TiO_2 of 61%.

3.4. Influence of promoters on SCR activity in the presence of water and oxygen

Six percent of H_2O was introduced into the feed to check the influence of water on NO_x reduction activity. We observed that the NO removal efficiency under dry conditions is higher than wet conditions at a low temperature region on both V_2O_5/TiO_2 and metal promoted V_2O_5/TiO_2 catalysts. This result agrees with the view of most researchers [29–31]. The activity at higher temperatures is not changed above 250 °C and the NO_x conversion obtained nearly 100%. The activity in the low temperature range of 150–250 °C was decreased to some extent because of competitive adsorption of H_2O and the reactants, NH_3 and/or NO, but the catalyst is not deactivated. Fig. 4 indicates the water effect on the NO_x reduction for the V_2O_5/TiO_2 and different metal promoted V_2O_5/TiO_2 catalysts. Among all the catalysts the NO_x conversion of V_2O_5/TiO_2, Se, Sb, Cu and S promoted V_2O_5/TiO_2 catalysts followed an order of Se > Sb > S > V_2O_5/TiO_2 > Cu similarly as in dry conditions (Fig. 3) but varied in percent conversion which are seems to be slightly less in efficiency in presence of water. Even though selenium (Se) is best promoter for NO_x conversion but its usage is limited because of its high vapor pressure, hence antimony (Sb) was taken as the best promoter. The V_2O_5/TiO_2

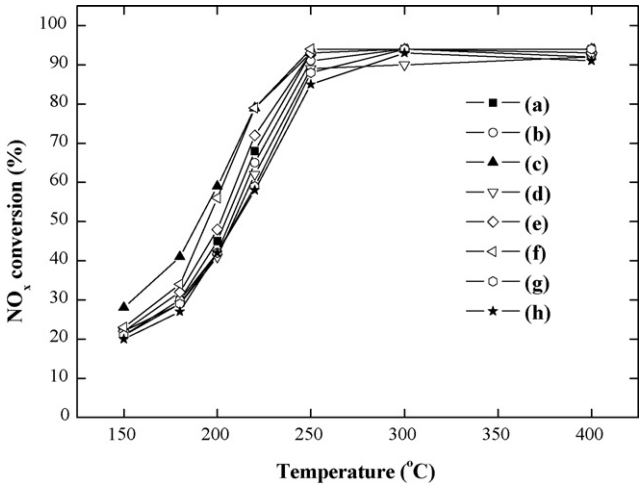

Fig. 4. NO_x conversion vs. temperature over (a) V_2O_5/TiO_2, (b) 1% $Cu/V_2O_5/TiO_2$, (c) 1% $Se/V_2O_5/TiO_2$, (d) 1% $Pb/V_2O_5/TiO_2$, (e) 1% $S/V_2O_5/TiO_2$, (f) 1% $Sb/V_2O_5/TiO_2$, (g) 1% $B/V_2O_5/TiO_2$ and (h) 1% $P/V_2O_5/TiO_2$ (conditions: 800 ppm NO_x, 800 ppm NH_3, 3 vol% O_2, 6 vol% H_2O; S.V.—60,000 h^{-1}).

catalyst obtained 45% conversion at a low temperature of 200 °C where as $Se/V_2O_5/TiO_2$ catalyst obtained 59% of conversion and $Sb/V_2O_5/TiO_2$ of 56%. Fig. 5 shows the different percentages of antimony promoted V_2O_5/TiO_2 catalysts in the presence of water. Among 1, 2, 3% $Sb/V_2O_5/TiO_2$ catalysts the 2% $Sb/V_2O_5/TiO_2$ showed high activity. With the increasing amount of antimony the low temperature activity enhanced up to the 2%. However, activity decreased with further addition of antimony more than 2%. When the amount of antimony is more than 3%, activity was even poorer than that of the V_2O_5/TiO_2 catalyst, which does not contain antimony. It seems that antimony covers the vanadia as well as TiO_2 when the amount of antimony is higher than 2%. Therefore, it can be observed that optimum amount of antimony is around 2%, which has high dispersion.

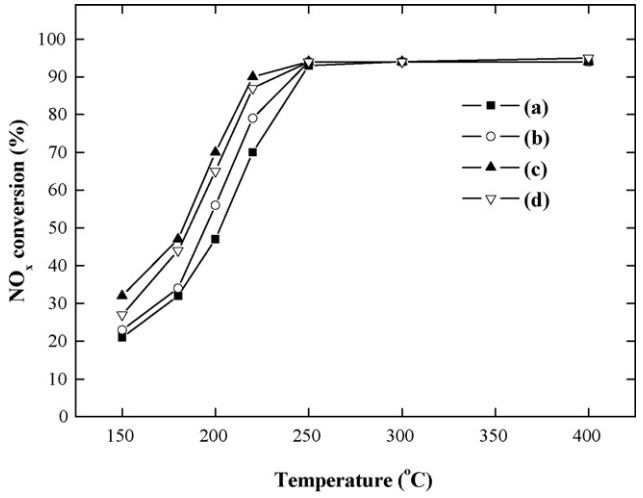

Fig. 5. NO_x conversion vs. temperature over (a) V_2O_5/TiO_2, (b) 1% $Sb/V_2O_5/TiO_2$, (c) 2% $Sb/V_2O_5/TiO_2$ and (d) 3% $Sb/V_2O_5/TiO_2$ (conditions: same as in Fig. 4).

3.5. Electrical conductivity study

It has been reported that NO_x conversion is closely related to the behavior of labile oxygen [27,32,33] which will be responsible for increase of electrical conductivities over the catalyst surfaces by the production of anionic vacancies which will be further responsible to react with surrounding anionic pollutants prevailing by introduction of reaction mixture gases during SCR reaction.

Therefore, it is thought that the difference in electrical conductivity (ΔG) over the catalysts surface, before and after introduction of reaction mixture gases could be the measure of an amount of labile oxygen activation. Hence electrical conductivity measurement studies were carried out for both the Sb(2%) and W(10%) promoted catalysts and their NO_x conversion efficiencies were compared at temperatures between 150 and 300 °C correlating with the obtained ΔG values.

Table 3 shows that the electrical conductivity increases with temperature. This indicates that the samples are in semi-conducting temperature region where conduction takes place mainly through the excitation of electrons at impurity levels. The excitation of electrons is promoted as temperature increases. The electrical conductivity values of Sb(2%)/V_2O_5/TiO_2 and W(10%)V_2O_5/TiO_2 catalysts at different temperatures were measured. It gives an important evidence of higher ΔG value for Sb(2%) promoter catalyst than for W(10%) promoted catalyst at low temperature (230 °C) which also gives well supported reason for the high conversion rates of Sb(2%)/V_2O_5/TiO_2 catalyst than that of commercial W(10%)V_2O_5/TiO_2 catalyst.

3.6. Low temperature SO_2 deactivation studies

In order to determine deactivation characteristics, NO_x conversions were measured with the introduction of 500 ppm SO_2 along with 800 ppm of NO, 800 ppm of NH_3, 6% H_2O and 3% O_2. The low temperature SO_2 deactivation studies were carried out for the metal promoted V_2O_5/TiO_2 catalysts which showed high NO_x conversions. Among the several metal promoted catalysts Se, Sb, Cu and S showed high NO_x conversions. The SO_2 deactivation studies were performed at 240 °C and the Se, Sb, Cu and S promoted catalysts were compared with V_2O_5/TiO_2 catalyst. Fig. 6 explains the effect of SO_2 on NO_x reduction over Se, Sb, Cu, and S promoted V_2O_5/TiO_2 catalysts and V_2O_5/TiO_2. The SO_2 deactivation is more serious on the copper (Cu) promoted catalyst than other catalysts as Cu can easily form the $CuSO_4$ which enhances the formation and existence of high amounts of ammonium bisulfate salts hence high deactivation occurred. This is in agreement with the order of bonding energy (M···O) of the metal promoters (Cu > Sb > Se > S) described in Section 3.1. Selenium catalysts also showed deactivation after 4 h because of its high vapor pressure. Best performance was obtained over antimony (Sb) promoted catalyst than the V_2O_5/TiO_2 catalyst. The amount of unreacted ammonia becomes very small and the amount of emitted sulfur dioxide is nearly similar to the amount

Table 3
ΔG and $\%NO_x$ conversions of $W/V_2O_5/TiO_2$ and $Sb/V_2O_5/TiO_2$ catalysts with temperature

Catalyst	Temperature (°C)	Electrical conductivity ($m^{-1}\ \Omega^{-1}$)		ΔG	$\%NO_x$ conversion
		Before gas supply	After gas supply		
$W/V_2O_5/TiO_2$	180	1.6×10^{-11}	2.0×10^{-10}	1.8×10^{-10}	45
	200	1.4×10^{-10}	8.0×10^{-10}	6.5×10^{-10}	54
	230	1.3×10^{-10}	9.6×10^{-10}	8.3×10^{-10}	77
	250	4.2×10^{-10}	3.0×10^{-9}	2.6×10^{-9}	100
	300	1.0×10^{-9}	3.8×10^{-8}	3.7×10^{-8}	100
$Sb/V_2O_5/TiO_2$	180	7.2×10^{-11}	3.0×10^{-10}	2.3×10^{-10}	50
	200	1.7×10^{-10}	9.2×10^{-10}	7.5×10^{-10}	61
	230	2.4×10^{-9}	1.5×10^{-9}	1.0×10^{-9}	89
	250	6.5×10^{-9}	9.4×10^{-8}	8.7×10^{-8}	100
	300	9.5×10^{-8}	9.8×10^{-7}	8.8×10^{-7}	100

introduced, it could be inferred that almost no oxidation of sulfur dioxide occurred within 16 h. This result clearly shows that antimony plays as a promoter enhancing the SO_2 poisoning resistance.

Fig. 7 shows the effect of antimony percentage on the SO_2 deactivation. With the addition of antimony, SO_2 deactivation is reduced and in all cases the antimony promoted catalyst showed best resistance to SO_2 deactivation than the V_2O_5/TiO_2 catalyst. The 2% $Sb/V_2O_5/TiO_2$ catalyst is optimized as it showed higher resistance to SO_2 deactivation than 1 and 3% of antimony catalysts up to 18 h. Increasing the percentage of antimony more than 2% caused decreasing the sulfur (SO_2) resistance. As shown in Fig. 8, deactivation starts early as the reaction temperature decreases to low temperatures. The V_2O_5/TiO_2 catalyst used to check the effect of SO_2 deactivation at low temperatures. When SO_2 deactivation study is carried at 220 °C the catalyst was poorly resistant to SO_2, but in the case of 240 and 250 °C the SO_2 resistant increased. At 220 °C the NO_x conversion is very low and the leftover ammonia can react easily with sulfur dioxide and water to favor the formation of ammonium bisulfate salt which can block the active sites and finally deactivates the catalyst.

Finally, sulfur (SO_2) deactivation behavior of $Sb(2\%)V_2O_5/TiO_2$ was compared with $W(10\%)V_2O_5/TiO_2$ commercial catalyst and SO_2 deactivation study was carried out at 230 °C for about 90 h and it was shown in Fig. 9. It is observed that the SO_2 resistance was higher for $Sb(2\%)V_2O_5/TiO_2$ than $W(10\%)V_2O_5/TiO_2$ catalyst. After 90 h of reaction the spent catalysts were analyzed by BET-SA, XPS and CHNS elemental analysis and the results found were correlated well with the deactivation behaviors of the catalysts.

The measured surface area values (Table 4) of fresh and spent catalysts of $W(10\%)V_2O_5/TiO_2$ and $Sb(2\%)V_2O_5/TiO_2$ also support the reason for decrease of catalytic activity [21] with decreasing the surface area of the catalysts. Surface area of the $W(10\%)V_2O_5/TiO_2$ catalyst reduced more than that of Sb(2%) promoted catalyst. This observation explains that the high catalytic activity of $Sb(2\%)V_2O_5/TiO_2$ than $W(10\%)V_2O_5/TiO_2$ at low temperatures is may be due to formation of higher amount of ammonium bisulfate salt over $W(10\%)V_2O_5/TiO_2$ than $Sb(2\%)V_2O_5/TiO_2$, causing more difference in reduction of surface area of $W(10\%)V_2O_5/TiO_2$ (Table 4).

The XPS spectra (Fig. 10(A and B)) obtained for the spent Sb(2%) and W(10%) promoted V_2O_5/TiO_2 catalysts are

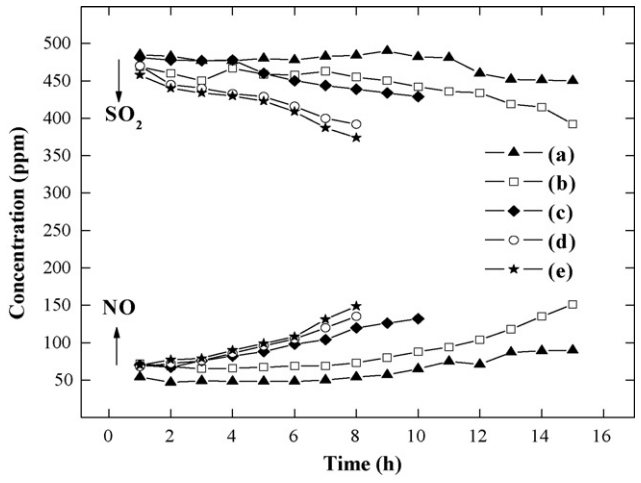

Fig. 6. SO_2 deactivation study at 240 °C over (a) 1% $Sb/V_2O_5/TiO_2$, (b) V_2O_5/TiO_2, (c) 1% $Se/V_2O_5/TiO_2$, (d) 1% $S/V_2O_5/TiO_2$ and (e) 1% $Cu/V_2O_5/TiO_2$ (conditions: 800 ppm NO_x, 800 ppm NH_3, 3 vol% O_2, 6 vol% H_2O, 500 ppm SO_2, S.V.—60,000 h^{-1}).

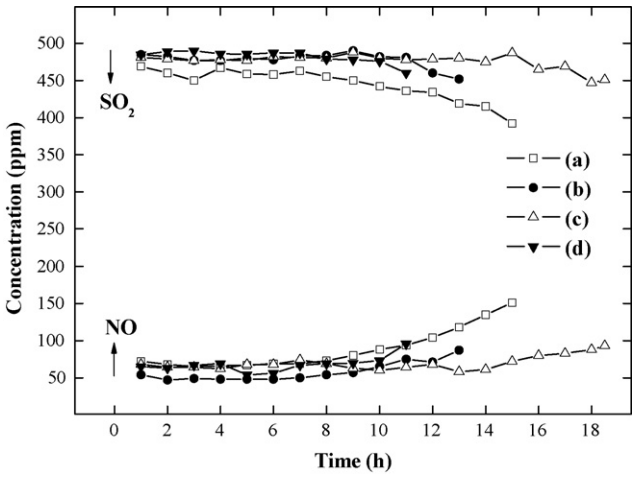

Fig. 7. SO_2 deactivation study at 240 °C over (a) V_2O_5/TiO_2, (b) 1% $Sb/V_2O_5/TiO_2$, (c) 2% $Sb/V_2O_5/TiO_2$ and (d) 3% $Sb/V_2O_5/TiO_2$ (conditions: same as in Fig. 6).

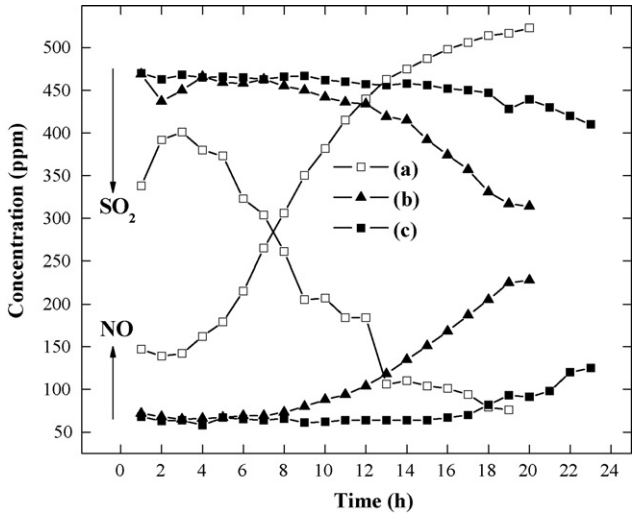

Fig. 8. SO_2 deactivation study over V_2O_5/TiO_2 catalysts at different temperatures (a) 220 °C, (b) 240 °C and (c) 250 °C (conditions: same as in Fig. 6).

Table 4
BET-SA of fresh and spent catalysts after 90 h of SO_2 deactivation

Catalyst	BET-SA (m^2g^{-1})	
	Fresh	After 90 h deactivation
$Sb(2\%)/V_2O_5/TiO_2$	89	62
$W(10\%)/V_2O_5/TiO_2$	85	45

showing the existence of ammonium bisulfate peaks, observed by the presence of S 2p spectra at binding energy of 168.2 eV [34] and N 1s spectra at binding energy of 401.8 eV [35]. The high intensities of the S 2p and N 1s peaks for commercial $W(10\%)V_2O_5/TiO_2$ catalyst observed from the XPS spectra confirming that the existence of high amount of ammonium bisulfates over the catalyst surface than the $Sb(2\%)V_2O_5/TiO_2$ catalyst. It is also confirmed by high atomic weight percentages of nitrogen and sulfur over $W(10\%)V_2O_5/TiO_2$ catalyst surface obtained through XPS analysis (Table 5).

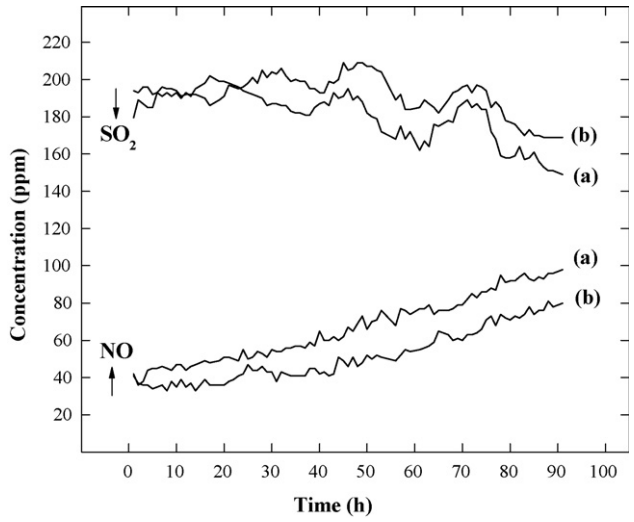

Fig. 9. SO_2 deactivation study at 230 °C over (a) $W(10\%)/V_2O_5/TiO_2$ and (b) $Sb(2\%)/V_2O_5/TiO_2$ (conditions: 200 ppm NO_x, 200 ppm NH_3, 3 vol% O_2, 12 vol% H_2O, 200 ppm SO_2, S.V.—60,000 h^{-1}).

Table 5
Atomic weight percentages of ammonium bisulfate salt formed after 90 h SO_2 deactivation

Catalyst	S (wt%)		N (wt%)		H (wt%)
	CHNS	XPS	CHNS	XPS	CHNS
$W(10\%)/V_2O_5/TiO_2$	5.07	4.53	4.83	4.42	1.75
$Sb(2\%)/V_2O_5/TiO_2$	2.97	2.54	2.21	2.04	1.02

The sulfur, nitrogen, hydrogen contents were measured from the CHNS elemental analysis for spent catalysts and the values are given in Table 5. The weight percentages of sulfur, nitrogen, hydrogen were higher for the $W(10\%)V_2O_5/TiO_2$ catalysts than the $Sb(2\%)V_2O_5/TiO_2$ catalyst which eventually supports the existence of high amount of ammonium bisulfate salt over $W(10\%)V_2O_5/TiO_2$ catalyst resulting in less resistance to sulfur (SO_2) deactivation [21,23]. Consequently it can be concluded that large amount of tungsten promoter can be replaced by smaller amount of antimony for the low temperature and/or sulfur environment application.

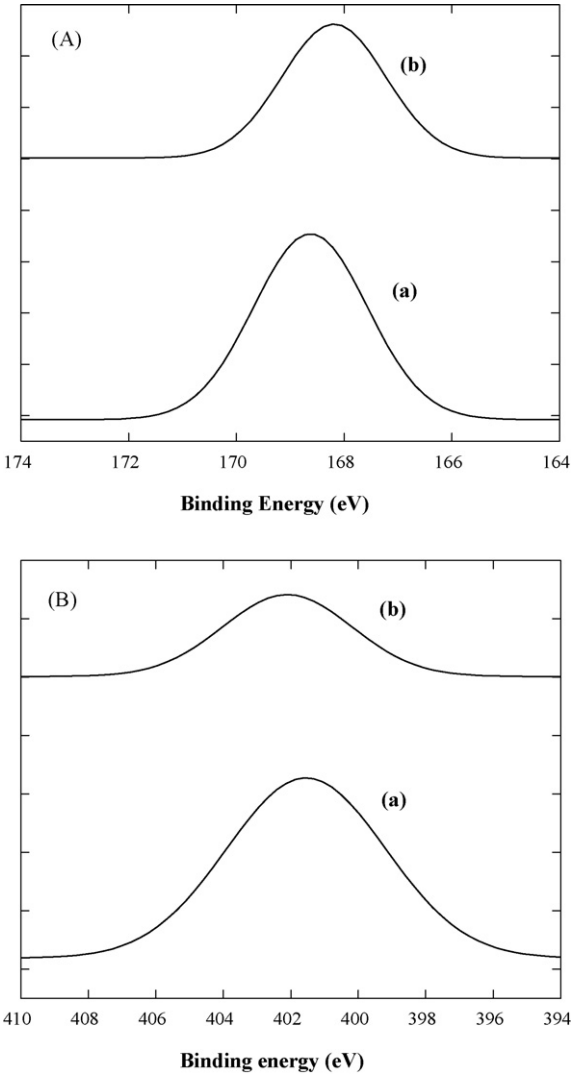

Fig. 10. XPS spectra of (A) S 2p and (B) N 1s of SO_2 deactivation samples after 90 h (a) $W/V_2O_5/TiO_2$ and (b) $Sb/V_2O_5/TiO_2$.

4. Conclusions

Quantum chemical calculation study was carried out to select promoters which are capable of decreasing SO_2 deactivation on V_2O_5/TiO_2 catalysts. Among the selected promoters selenium, antimony, copper and sulfur showed for high NO_x conversions at low temperatures. From the sulfur deactivation studies it is concluded that antimony promoted V_2O_5/TiO_2 catalyst is best for the low temperature SO_2 deactivation resistance. The high electrical conductivity change (ΔG) of $Sb(2\%)V_2O_5/TiO_2$ than $W(10\%)V_2O_5/TiO_2$ catalyst obtained during in situ electrical conductivity study and its correlation with high catalytic activity at low temperatures suggest that the $Sb(2\%)V_2O_5/TiO_2$ is highly promising catalyst. The evidences and interpretations observed by the XPS, BET-SA and CHNS elemental analysis also confirmed the effective catalytic performance and resistance to SO_2 of $Sb(2\%)V_2O_5/TiO_2$ than $W(10\%)V_2O_5/TiO_2$ at low temperatures. Finally it is concluded that $Sb(2\%)$ promoted V_2O_5/TiO_2 catalyst can be efficiently used as sulfur resistance catalyst at low temperatures in substitution to commercial $W(10\%)V_2O_5/TiO_2$.

Acknowledgements

This research work was supported by a grant (07K1501-01812) from 'Center for Nanostructured Materials Technology' under '21st Century Frontier R&D Programs' of the Ministry of Science and Technology, Korea.

References

[1] H. Bosch, F. Janssen, Catal. Today 2 (1988) 369–379.
[2] J.G. Henry, G.W. Heinke, Environmental Science and Engineering, Prentice-Hall, Englewood Cliffs, NJ, 1989.
[3] F. Luck, J. Roiron, Catal. Today 4 (1989) 205–218.
[4] P.G. Smirniotis, D.A. Peña, B.S. Uphade, Angew. Chem. Int. Ed. 40 (2001) 2479–2482, and references therein.
[5] F. Nozaki, K. Yamazaki, T. Inomata, Chem. Lett. (1977) 521–524.
[6] L. Singoredjo, M. Slagt, J. van Wees, F. Kapteijn, J.A. Moulijn, Catal. Today 7 (1990) 157–165.
[7] L. Singoredjo, R. Korver, F. Kapteijn, J.A. Moulijn, Appl. Catal. B 1 (1992) 297–316.
[8] Z. Zhu, Z. Liu, S. Liu, H. Niu, Appl. Catal. B 30 (2001) 267–276.
[9] H.E. Curry-Hyde, H. Musch, A. Baiker, Appl. Catal. 65 (1990) 211–223.
[10] S. Kasaoka, E. Sasaoka, H. Iwasaki, Bull. Chem. Soc. Jpn. 62 (1989) 1226–1232.
[11] Z. Zhu, Z. Liu, S. Liu, H. Niu, T. Hu, T. Liu, Y. Xie, Appl. Catal. B 26 (2000) 25–35.
[12] M. Yoshikawa, A. Yasutake, I. Mochida, Appl. Catal. A 173 (1998) 239–245.
[13] L. Singoredjo, R. Korver, F. Kapteijn, J.A. Moulijn, Appl. Catal. B 10 (1996) 237–243.
[14] H. Schneider, M. Maciejewski, K. Köhler, A. Wokaun, A. Baiker, J. Catal. 157 (1995) 312–320.
[15] J. Blanco, P. Avila, S. Suárez, J.A. Martín, C. Knapp, Appl. Catal. B 28 (2000) 235–244.
[16] D.A. Peña, B.S. Uphade, P.G. Smirniotis, J. Catal. 221 (2004) 421–431.
[17] X. Tang, J. Hao, W. Xu, J. Li, Catal. Commun. 8 (2007) 329–334.
[18] I.-S. Nam, J.W. Eldridge, J.R. Kittrell, Ind. Eng. Chem. Prod. Res. Dev. 25 (1986) 192–197.
[19] S.T. Choo, S.D. Yim, I.-S. Nam, S.-W. Ham, J.-B. Lee, Appl. Catal. B 44 (2003) 237–252.
[20] J.W. Choung, I.-S. Nam, S.-W. Ham, Catal. Today 111 (2006) 242–247.
[21] Z. Huang, Z. Zhu, Z. Liu, Appl. Catal. B 39 (2002) 361–368.
[22] Z. Huang, Z. Zhu, Z. Liu, Q. Liu, J. Catal. 214 (2003) 213–219.
[23] S.-w. Ham, H. Choi, I.-S. Nam, Y.G. Kim, Catal. Today 11 (1992) 611–621.
[24] M. Najbar, E. Brocławik, A. Góra, J. Camra, A. Białas, A.W. Birczyńska, Chem. Phys. Lett. 325 (2000) 330–339.
[25] G. Madia, M. Elsener, M. Koebel, F. Raimondi, A. Wokaun, Appl. Catal. B 39 (2002) 181–190.
[26] C. Orsenigo, L. Lietti, E. Tronconi, P. Forzatti, F. Bregani, Ind. Eng. Chem. Res. 37 (1998) 2350–2359.
[27] J.M. Herrmann, J. Disdier, Catal. Today 56 (2000) 389–401.
[28] Z. Zhu, H. Niu, Z. Liu, S. Liu, J. Catal. 195 (2000) 268–278, and references therein.
[29] M.D. Amirids, I.E. Wachs, G. Deo, J.-M. Jehng, D.S. Kim, J. Catal. 161 (1996) 247–253.
[30] M.D. Amirids, R.V. Duevel, I.E. Wachs, Appl. Catal. B 20 (1999) 111–122.
[31] Chia-Hsin, H. Bai, Ind. Eng. Chem. Res. 43 (2004) 5983–5988.
[32] R.B. Bjorklund, C.U.I. Odenbrand, J.G.M. Brandin, L.A.H. Andersson, B. Liedberg, J. Catal. 119 (1989) 187–200.
[33] R.B. Bjorklund, L.A.H. Anderson, C.U.I. Odenbrand, L. Sjöqvist, A. Lund, J. Phys. Chem. 96 (1992) 10953–10959.
[34] A.A. Audi, P.M.A. Sherwood, Surf. Interface Anal. 29 (2000) 265–275.
[35] J.F. Moulder, W.F. Stickle, P.E. Sobol, K.D. Bomben, Handbook of X-ray Photoelectron Spectroscopy, Perkin-Elmer, Eden Prairie, 1992.